



UDC 621.762

<https://doi.org/10.17073/1997-308X-2024-2-23-34>Research article
Научная статья

Phase composition, structure and properties of B₄C–TiB₂ ceramics produced by hot pressing

R. R. Khabirov¹✉, N. Yu. Cherkasova¹, T. S. Gudyma¹, Yu. L. Krutskii¹,
A. V. Mass¹, T. S. Ogneva¹, R. I. Kuzmin¹, A. G. Anisimov²

¹Novosibirsk State Technical University

20 Karl Marx Prosp., Novosibirsk 630073, Russia

²Lavrentyev Institute of Hydrodynamics of Siberian Branch of Russian Academy of Sciences

15 Academician Lavrentiev Prosp., Novosibirsk 630090, Russia

✉ xabirov.2016@stud.nstu.ru

Abstract. Composite ceramic materials based on B₄C with the addition of TiB₂ in amounts of 0, 10, 20, 25 and 30 mol. % have been studied. Titanium diboride was synthesized from TiO₂ powder and nanofibrous carbon using the boron carbide method in an induction furnace at 1650 °C in an argon atmosphere. The samples were produced by hot pressing at 2100 °C and 25 MPa in an argon environment. The phase composition was determined, and the apparent density and open porosity of the experimental materials were measured. The microstructure was assessed using optical and scanning electron microscopy. The investigations revealed that an increase in the TiB₂ content reduces the open porosity while concurrently enhancing the relative density of the boron carbide ceramics. For a sample containing 30 mol. % TiB₂, the open porosity and relative theoretical density were 1.6 and 99 %, respectively. Using XRD and XRS analyses established that the synthesized materials are comprised of two phases: B₄C and TiB₂. The average grain size of TiB₂ was 0.85 ± 0.02 μm for the sample with 10 mol. % TiB₂ and 8.90 ± 0.25 μm for the material with 30 mol. % TiB₂. It was found that at higher TiB₂ concentrations, large clusters of grains are formed. The destruction pattern of B₄C grains is intragranular, while TiB₂ grains are characterized by intergranular destruction. For a sample containing 30 mol. % TiB₂, the fracture toughness was 4.97 ± 0.23 MPa·m^{0.5}, and the hardness was 3320 ± 120 HV_{0.5}. Therefore, the addition of TiB₂ at these specified concentrations facilitated a 30 % enhancement in fracture toughness relative to single-phase B₄C while preserving a high level of hardness.

Keywords: composite ceramics, B₄C, TiB₂, fracture toughness, crack deflection

Acknowledgements: The research was conducted at the core facility “Structure, mechanical and physical properties of materials”, NSTU (No. 13. TsKP.21.0034, 075-15-2021-698).

For citation: Khabirov R.R., Cherkasova N.Yu., Gudyma T.S., Krutskii Yu.L., Mass A.V., Ogneva T.S., Kuzmin R.I., Anisimov A.G. Phase composition, structure and properties of B₄C–TiB₂ ceramics produced by hot pressing. *Powder Metallurgy and Functional Coatings*. 2024;18(2):23–34. <https://doi.org/10.17073/1997-308X-2024-2-23-34>

Фазовый состав, структура и свойства B_4C - TiB_2 -керамики, полученной горячим прессованием

Р. Р. Хабиров¹✉, Н. Ю. Черкасова¹, Т. С. Гудыма¹, Ю. Л. Крутский¹,
А. В. Масс¹, Т. С. Огнева¹, Р. И. Кузьмин¹, А. Г. Анисимов²

¹Новосибирский государственный технический университет
Россия, 630073, г. Новосибирск, пр-т Карла Маркса, 20

²Институт гидродинамики им. М.А. Лаврентьева СО РАН
Россия, 630090, г. Новосибирск, пр-т Академика Лаврентьева, 15

✉ xabirov.2016@stud.nstu.ru

Аннотация. Исследованы композиционные керамические материалы на основе B_4C с добавлением TiB_2 в количестве 0, 10, 20, 25, 30 мол. %. Диборид титана был синтезирован из порошка TiO_2 и нановолокнистого углерода карбидоборным методом в индукционной печи при температуре 1650 °С в потоке аргона. Образцы получены методом горячего прессования при температуре 2100 °С и давлении 25 МПа в атмосфере аргона. Определен фазовый состав и измерены кажущаяся плотность и открытая пористость экспериментальных материалов. Микроструктуру оценивали методами оптической и растровой электронной микроскопии. Выявлено, что увеличение содержания TiB_2 снижает открытую пористость и увеличивает относительную плотность керамики на основе карбида бора. Для образца, содержащего 30 мол. % TiB_2 , открытая пористость и относительная от теоретической плотность составили 1,6 % и 99 % соответственно. Методами рентгенофазового и микрорентгеноспектрального анализов установлено, что полученные материалы состоят из двух фаз – B_4C и TiB_2 . Средний размер зерен TiB_2 составил $0,85 \pm 0,02$ мкм для образца с 10 мол. % TiB_2 и $8,90 \pm 0,25$ мкм для материала с 30 мол. % TiB_2 . Установлено, что при более высокой концентрации TiB_2 образуются крупные скопления зерен. Характер разрушения B_4C -зерен – внутривершинный, а для TiB_2 -зерен характерно межзеренное разрушение. Для образца, содержащего 30 мол. % TiB_2 , трещиностойкость составила $4,97 \pm 0,23$ МПа·м^{0,5}, твердость – 3320 ± 120 HV_{0,5}. Таким образом, добавка TiB_2 в таком количестве позволила увеличить трещиностойкость на 30 % по сравнению с однофазным B_4C и сохранить высокий уровень твердости.

Ключевые слова: композиционная керамика, B_4C , TiB_2 , трещиностойкость, отклонение трещины

Благодарности: Исследования проведены на оборудовании ЦКП «Структура, механические и физические свойства материалов» НГТУ. (№ 13.ЦКП.21.0034, 075-15-2021-698).

Для цитирования: Хабиров Р.Р., Черкасова Н.Ю., Гудыма Т.С., Крутский Ю.Л., Масс А.В., Огнева Т.С., Кузьмин Р.И., Анисимов А.Г. Фазовый состав, структура и свойства B_4C - TiB_2 -керамики, полученной горячим прессованием. *Известия вузов. Порошковая металлургия и функциональные покрытия*. 2024;18(2):23–34. <https://doi.org/10.17073/1997-308X-2024-2-23-34>

Introduction

Ceramics based on B_4C are garnering significant interest from the research community due to their distinct combination of properties, including a high level of hardness (50 GPa) and low density (2.52 g/cm³), positioning them as a promising candidate for the fabrication of sandblasting nozzles [1–3].

Achieving a density in B_4C ceramics that approximates the theoretical maximum is challenging due to the presence of strong covalent B–C bonds, a low self-diffusion coefficient, and substantial resistance to grain boundary slippage. B_4C also presents limitations in terms of its relatively modest fracture toughness (3.1–3.2 МПа·м^{0.5}) [4] and bending strength (475–579 МПа) [5].

Suppressing the growth of B_4C grains through the establishment of a two-phase structure has been shown to enhance sintering conditions, thereby facilitating the production of ceramics with a relative den-

sity nearing the theoretical ideal [6; 7]. Furthermore, the development of composite materials derived from boron carbide impacts the pattern of destruction. Introducing dispersed particles that exhibit greater plasticity into the B_4C matrix promotes the dissipation of crack energy within the ceramics [8], culminating in an increase in material fracture toughness [9].

Titanium diboride is frequently utilized as an additive that favorably influences the characteristics of B_4C ceramics. The B_4C - TiB_2 system is characterized by an absence of significant mutual solubility, with TiB_2 establishing a mechanical mixture alongside B_4C . A composition comprising 75–78 mol. % B_4C and 22–25 mol. % TiB_2 aligns with a eutectic point that has a melting temperature of 2200 °C [10; 11]. Consequently, the sintering process for the B_4C - TiB_2 composite material is executed at a reduced temperature, resulting in a structure that features isolated TiB_2 grains dispersed throughout a polycrystalline B_4C matrix [12]. The coefficients of linear thermal expansion for titanium boride

and boron carbide are markedly different ($5.5 \cdot 10^{-6} \text{ }^\circ\text{C}^{-1}$ for B₄C, $7.8 \cdot 10^{-6} \text{ }^\circ\text{C}^{-1}$ for TiB₂) [13]. In this regard, in such materials, upon cooling after sintering, residual stresses arise, which, according to the authors of [14], reach 1 GPa. Therefore, upon cooling after sintering, residual stresses emerge within the material, which, as suggested by [14], can reach up to 1 GPa. Here, not only the magnitude but also the distribution of these stresses is of critical importance. Tensile stresses and microcracks tend to form along the grain boundaries, whereas the compressive stresses within B₄C crystallites act to inhibit their growth and the subsequent development of macrocracks [15]. This stress distribution significantly contributes to the elevated fracture toughness observed in these ceramics [16; 17].

B₄C–TiB₂ composites produced via hot pressing (HP) attain a relative density of 99.8 % and a fracture toughness of $9.4 \text{ MPa}\cdot\text{m}^{0.5}$, albeit with a slight reduction in hardness (26 GPa) when contrasted with additive-free B₄C [5; 14; 18–21]. It has been observed that the *in-situ* formation of titanium diboride within the material – arising from the synthesis of B₄C, TiB₂, and carbon during ceramic sintering – contributes to enhanced mechanical properties of the sintered composite relative to composites incorporating directly added TiB₂ powders [5; 14; 22]. Nevertheless, the mechanisms governing the evolution of the microstructure of B₄C ceramics with varying concentrations of TiB₂ additive, as well as its impact on the properties of the composites, remain insufficiently elucidated in the literature.

In the studies reported in [6], the properties and microstructure of B₄C ceramics were analyzed in correlation with the concentration of the TiB₂ additive. An increase in fracture toughness was observed with an increase in TiB₂ content beyond 10 %; however, the incorporation of more than 30 mol. % TiB₂ resulted in diminished hardness and bending strength, attributable to the intrinsically lower strength attributes of TiB₂. Additionally, an elevated TiB₂ content exceeding 30 mol. % was correlated with a decrease in the composite's relative density [12; 23], potentially due to TiB₂ limited sinterability [6].

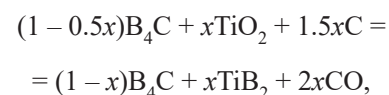
In the current research, TiB₂ was synthesized through the boron carbide method using B₄C, TiO₂, and a carbonaceous agent. Typically, acetylene black with a specific surface area (S_{sp}) of approximately $50 \text{ m}^2/\text{g}$ is utilized as a carbon source in the synthesis of refractory oxygen-free compounds. In this instance, nanofibrous carbon, also with an S_{sp} of around $50 \text{ m}^2/\text{g}$, was employed. The use of carbon materials with an expansive specific surface area is known to expedite solid-phase reactions, hence their application represents a promising avenue in the exploration of methodologies for synthesizing composite ceramics [24].

The objective of this study is to delineate the patterns in the formation of phase composition, microstructure, and properties of B₄C composite ceramics that incorporate TiB₂ synthesized with the aid of nanofibrous carbon.

Materials and methods

Highly dispersed B₄C powders (98.5 % purity, 2.1 μm particle size), synthesized according to the method given in [25], TiO₂ (99 % purity, 1 μm particle size) and nanofibrous carbon (99 % purity) were utilized as the initial components. The latter consisted of granules 0.4–8.0 mm in size, which were composed of intertwined fibers with an average diameter of 73 nm, and was produced by the catalytic decomposition of natural and hydrocarbon gases [26]. To enhance reactivity, the nanofibrous carbon granules were pre-milled in an AGO-2S planetary mill for 5 min at an acceleration of 15g and a ball-to-material weight ratio of 15:1. The drums and milling media were made of ZrO₂. The average particle size of the nanofibrous carbon granules post-milling was 3.9 μm. The proportions of the initial powders in the mixture were calculated to facilitate the formation of 10, 20, 25 and 30 mol. % TiB₂ in the sintered ceramics. Samples of B₄C without additives were also prepared.

The composition of the powder mixtures was determined based on an analysis published data. Titanium diboride was synthesized in a solid phase reaction using the boron carbide method [27], according to the following reaction [22]



where x is the mole fraction of TiB₂ in the mixture.

The mixing of boron carbide, titanium oxide, and nanofibrous carbon powders occurred in an AGO-2S planetary mill for 5 min at an acceleration of 20g, using a ball-to-material weight ratio of 30:1. Only powders that had been sieved through a 100 μm mesh were used. The synthesis of TiB₂ was performed in an indirect heating induction furnace under an argon atmosphere at 1650 °C, with a dwell time of 20 min. The median particle sizes (d_{50}) for the synthesized powders containing 10, 20, 25 and 30 mol. % TiB₂ were 7.4, 8.3, 8.4 and 13.4 μm, respectively.

The synthesized powders were employed to fabricate samples by hot pressing (HP) at 2100 °C under a pressure of 25 MPa in an argon atmosphere. The HP process lasted for 70 min, with a dwell time at the maximum temperature of 25 min. The dimensions of the sintered samples were 20 mm in diameter and 4 mm in height. The HP parameters were chosen with consideration

of published findings. For instance, research detailed in [28] indicates that a HP temperature of 2100 °C yields the highest relative density in ceramics. Other studies [29; 30] have also conducted hot pressing of B_4C ceramics at this temperature.

Diffraction patterns were captured using an ARL X'TRA diffractometer (Thermo Scientific, Switzerland) equipped with a θ – θ goniometer. The end surfaces of the samples which had been cleared of any residues from the graphite paper used as a separator during the hot pressing process, were photographed after a meticulous grinding process.

The phase composition was determined utilizing the corundum number method. A profile analysis of the diffraction pattern was carried out in the Fityk software package (Poland) to assess the integral intensity of the largest phase peaks. The weight fraction of the phases was calculated according to the formula

$$w_k = \frac{\frac{I_k^{\max}}{RIR_k}}{\sum \frac{I_i^{\max}}{RIR_k}},$$

where I_k^{\max} is the integral intensity of the largest peak of the given phase, RIR_k is the corundum number of that phase.

The apparent density and open porosity of the ceramics were measured by hydrostatic weighing. The relative density was determined as the ratio of the apparent density to the theoretical value:

$$\rho_{\text{rel}} = \frac{\rho_{\text{app}}}{\rho_{\text{theor}}} \cdot 100 \text{ \%}.$$

The theoretical density for each composite was calculated using the rule of mixtures, referencing the X-ray density values of the components found in the literature B_4C (2.5 g/cm³) and TiB_2 (4.5 g/cm³) [31–33].

The average particle size of the powder was determined using a MicroSizer 201 VA Instrument laser particle size analyzer (VA Instalt, Russia). Microstructural examination was performed on polished sections and fracture surfaces employing EVO 50 optical and scanning electron microscopes (Carl Zeiss, Germany). To enhance the electrical conductivity of the samples under investigation, a copper layer approximately 20 nm in thickness was sputtered onto the polished surfaces. The chemical composition of the samples was analyzed through energy dispersive X-ray spectroscopy (EDX) using the INCA X-ACT system, and maps depicting the distribution of chemical elements were generated.

Hardness and fracture resistance measurements were conducted utilizing a 402MVD hardness tester (Wolpert Group, Germany) equipped with a diamond tetrahedral Vickers pyramidal indenter. Hardness was measured by the Vickers method under an indenter load of 500 g, while fracture toughness tests were administered with a load of 5 kg. The values of this index were initially computed using various methods, inclusive of equations from [34; 35]. The utilization of equations that consider Young's modulus (E) yields more accurate values of the critical stress intensity factor (K_{Ic}), especially when investigating composite materials with significant discrepancies in E values. Employing simplified equations often results in overestimations that deviate substantially from actual values [36]. Consequently, most literature concentrating on the evaluation techniques for calculating the critical stress intensity factor use equations that include Young's modulus [34; 35]:

$$K_{Ic} = 0.048 \left(\frac{l}{a} \right)^{-0.5} \left(\frac{H_v}{E\phi} \right)^{-0.4} \frac{H_v a^{0.5}}{\phi},$$

where H_v is the hardness, GPa; l is the crack length, μm ; a is the indentation half diagonal, μm ; $\phi = 3$ is the constant.

The Young's modulus of the experimental materials was determined using the rule of mixtures:

$$E = \frac{100}{\frac{m_i}{E_i} + \frac{m_j}{E_j}},$$

where E_i and E_j are the Young's modulus values of B_4C and TiB_2 , respectively, GPa; m_i and m_j are their weight fractions, %.

For these calculations, the values of Young's modulus for hot-pressed B_4C (450 GPa) and TiB_2 (530 GPa) were taken from [31–33].

Results and discussion

Open porosity and density of composite ceramic materials

The study evaluated the impact of varying titanium diboride concentrations on the alteration of (ρ_{rel}) and open porosity (P). The findings are illustrated in Fig. 1. In the B_4C ceramics devoid of additives, a high ρ_{rel} was observed at $97.66 \pm 0.49 \text{ \%}$, with $P = 0.07 \pm 0.02 \text{ \%}$. These figures confirm the appropriateness of the selected hot pressing parameters, which facilitated the production of low-porosity ceramics.

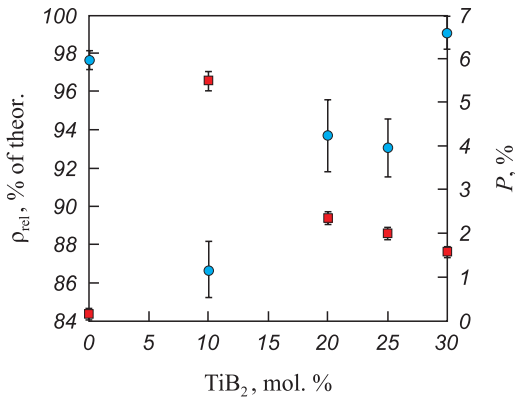


Fig. 1. Relative density (●) and open porosity (■) of experimental materials as a function of the amount of TiB₂ additive

Рис. 1. Относительная от теоретической плотность (●) и открытая пористость (■) экспериментальных материалов в зависимости от количества добавки TiB₂

Nevertheless, the sample containing 10 mol. % TiB₂ exhibited a lower prel and increased P.

With the escalation of TiB₂ content to 30 mol. %, there was a 15 % increase in relative density and a 42 % reduction in open porosity in comparison to the specimen with 10 mol. % TiB₂. The resulting material's relative density is on par with that of composite B₄C ceramics reported in other studies [6; 7; 37].

Phase analysis

Fig. 2 presents the X-ray diffraction pattern of a composite material consisting of boron carbide and 30 mol. % titanium diboride, which is characterized by the highest relative density. The sample's composition by weight percentage is: 65B₄C, 31TiB₂ and 4C.

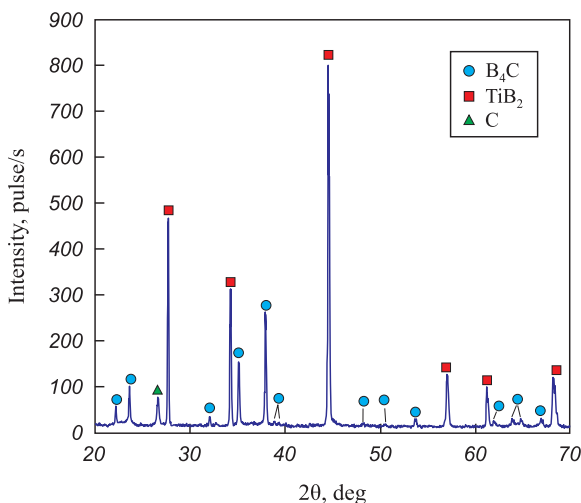


Fig. 2. XRD pattern of B₄C ceramic sample with 30 mol. % TiB₂

Рис. 2. Рентгеновская дифракционная картина образца керамики B₄C с 30 мол. % TiB₂

Graphite paper served as a barrier between the punch and the powder during hot pressing. It is possible that particles of the graphite penetrated into the more profound pores evident on the sample's surface. This could account for the carbon reflection observed in the diffraction pattern.

The lack of TiO₂ reflections in Fig. 2 suggests the complete reaction of the starting powder materials. Furthermore, the absence of ZrO₂ reflections implies that there was no significant attrition of the milling media during the milling process.

Microstructural study

The microstructure of composite ceramics with a 30 mol. % addition of TiB₂ comprises a matrix (appearing gray in images) interspersed with light-colored clusters of varying sizes (Fig. 3, a). To elucidate the consti-

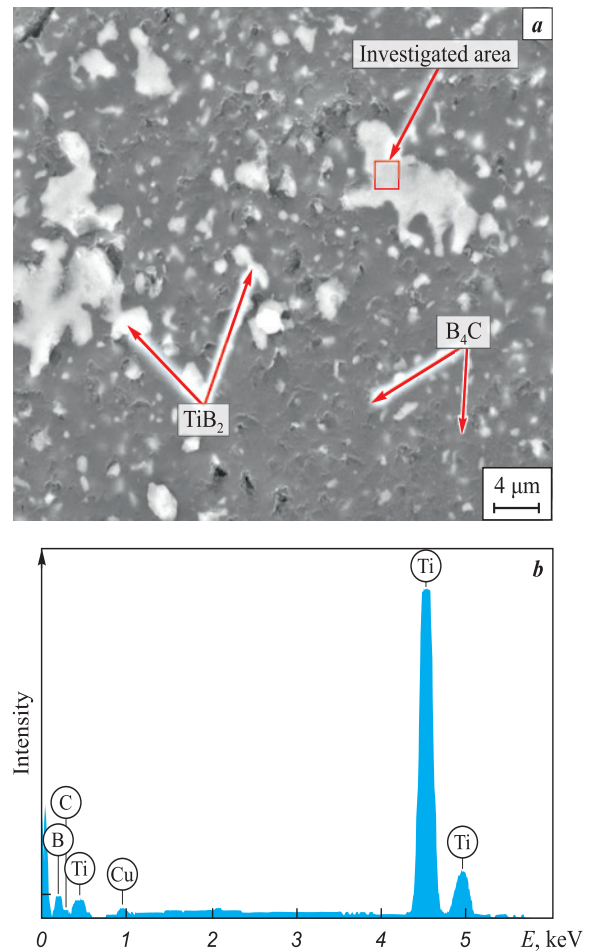


Fig. 3. Results of EDX analysis of ceramics containing 30 mol. % TiB₂

a – general view of the investigated area, b – EDX spectrum

Рис. 3. Результаты EDX-анализа керамики, содержащей 30 мол. % TiB₂

a – общий вид исследуемой области, b – характеристический рентгеновский спектр

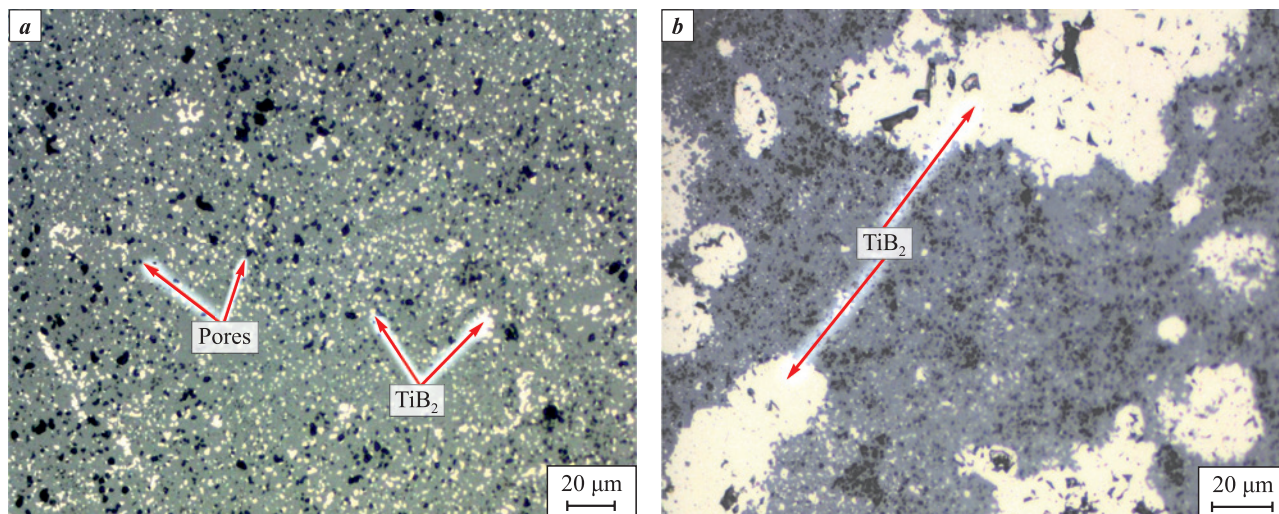


Fig. 4. Microstructure of B_4C samples with 10 mol. % (a) and 20 mol. % (b) TiB_2 additions

Рис. 4. Микроструктура образцов B_4C с добавкой TiB_2 в количестве 10 мол. % (a) и 20 мол. % (b)

tments of the structure, maps detailing the distribution of chemical elements were generated, and reflections indicative of boron and titanium were observed within these light clusters (Fig. 3, b). Consequently, these clusters have been identified as the TiB_2 phase. The absence of zirconium in the spectral analysis further corroborates the lack of significant wear on the grinding media during processing.

The material with 10 mol. % TiB_2 exhibits a low relative density and elevated open porosity, which is attributed to the large number of pores (Fig. 4, a). TiB_2 grains are evenly dispersed throughout the B_4C matrix. However, an increase in TiB_2 content is associated with the emergence of larger aggregates of this phase (Fig. 4, b).

Fig. 5 provides histograms that portray the distribution of TiB_2 grain size across composites of varying compositions, while an accompanying table lists their mean size (d_{avg}) along with the d_{50} and d_{90} statistics. The grain size distribution curves for the composite ceramics exhibit a unimodal configuration with a single pronounced peak. A lognormal function was employed to model the distribution curve of TiB_2 grain sizes in the fabricated materials.

With an increment in TiB_2 content within the material's composition, there is a corresponding increase in the average size of the diboride grains, as well as the formation of large clusters. In the specimen containing 10 mol. % TiB_2 , the largest grain clusters do not exceed 4.5 μm . The restricted range of size distribution in this

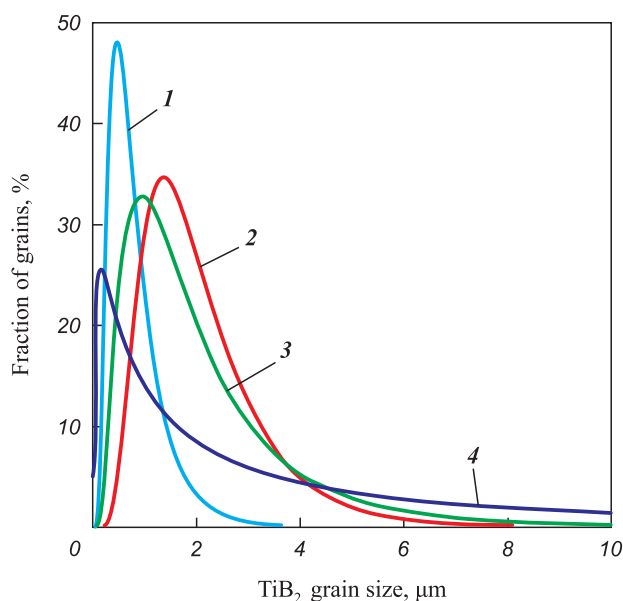


Fig. 5. Histogram plot of TiB_2 grain size distribution in sintered ceramics:

1 – 10 mol. % TiB_2 ; 2 – 20 mol. % TiB_2 ;
3 – 25 mol. % TiB_2 ; 4 – 30 mol. % TiB_2

Рис. 5. Участок гистограммы распределения размера зерен TiB_2 в спеченной керамике:

1 – 10 мол. % TiB_2 ; 2 – 20 мол. % TiB_2 ;
3 – 25 мол. % TiB_2 ; 4 – 30 мол. % TiB_2

**Average size and parameters
 d_{50}, d_{90} of TiB_2 grains
in $B_4C + TiB_2$ ceramic samples**

**Средний размер и параметры
 d_{50}, d_{90} зерен TiB_2 в образцах
композиционной керамики $B_4C + TiB_2$**

TiB_2 , mol. %	d_{avg} , μm	d_{50} , μm	d_{90} , μm
10	0.85 ± 0.02	0.72	1.37
20	2.05 ± 0.04	1.62	3.47
25	2.40 ± 0.09	1.40	5.26
30	8.90 ± 0.25	1.82	35.89

ceramic suggests a uniform growth of the second phase inclusions. Conversely, clusters measuring up to 320 μm were identified in the sample with 30 mol. % TiB₂. The distribution function graph for the TiB₂ grain sizes in this sample demonstrates an asymmetrical profile, with a considerable presence of coarse grains, as indicated by the elevated d_{90} values. Meanwhile, the d_{50} parameter shows only a minor increase with the rise in TiB₂ concentration. Therefore, the microstructure of the ceramics is characterized by a combination of uniformly distributed fine TiB₂ grains and larger grains and clusters. This phenomenon is likely due to the high degree of agglomeration present in the initial powder mixtures and the subsequent growth of these agglomerates during the TiB₂ synthesis process.

Microstructural images from studies [18; 23] also affirm that the size of grain clusters for this phase expands as the TiB₂ concentration increases. Findings by researchers in [38] demonstrate that employing finer B₄C powder aids in creating fine-grained B₄C–TiB₂ ceramics with a more homogeneously distributed TiB₂ phase.

To mitigate the inhomogeneity of the grain structure, it is advisable to extend the milling duration of the powder mixtures prior to the synthesis of TiB₂ powder, and also to perform additional milling of the synthesized powder mixture.

Mechanical properties

The incorporation of TiB₂, which possesses a lower hardness than B₄C, results in a decrease in the hardness of the B₄C–TiB₂ composite as depicted in Fig. 6 and corroborated by numerous studies [7; 15]. The diminished fracture toughness observed in samples containing 10, 20, and 25 mol. % TiB₂ additives is attributed to their high open porosity and low relative density. The presence of large pores within the ceramic matrix adversely affects its resistance to crack propagation [39]. Nevertheless, enhancing the TiB₂ content to 30 mol. % yielded improvements in both hardness and fracture toughness over materials with lesser additive amounts and the pure B₄C sample.

Research in [6] reported the fabrication of ceramics with 30 mol. % TiB₂ from commercial B₄C and TiB₂ powders through spark plasma sintering ($P = 50$ MPa, $t = 2000$ °C). The resultant material's relative density was 97.91 % of theoretical, with a hardness of 28.86 ± 0.29 GPa and fracture resistance of 4.36 ± 0.1 MPa·m^{0.5}, figures that are inferior to those achieved in the current study. The authors of [6] suggest that the decreased performance metrics with TiB₂ contents exceeding 5 mol. % are due to TiB₂'s limited sinterability. In contrast, our study demonstrates an increase in

the relative density of ceramics with rising TiB₂ concentrations, underscoring the enhanced sinterability of titanium diboride synthesized via the boron carbide method compared to that of commercial powders.

The research presented in [38] involved synthesizing ceramics using commercial powders of B₄C and 30 vol. % (37.5 mol. %) TiB₂ by hot pressing at 2000 °C and 35 MPa. This process produced a material with a uniform distribution of TiB₂ grains, a theoretical relative density of 100 %, and mechanical properties ($H_v = 30.42 \pm 0.79$ GPa, $K_{Ic} = 5.16 \pm 0.19$ MPa·m^{0.5}) comparable to those observed in the present study, likely facilitated by intensive milling for 12 h.

Similarly, [12] describes ceramics with 30 vol. % (37.5 mol. %) TiB₂ and 100 % relative density, prepared from commercial B₄C and TiB₂ powders subjected to 24 h of grinding and subsequently sintered by spark plasma sintering at 2000 °C and 60 MPa. This material exhibited a hardness of 31 ± 0.5 GPa and a fracture toughness of 3.75 ± 0.25 MPa·m^{0.5}.

These comparative analyses indicate that the mechanical properties of the experimental material developed in this work are competitive with those of ceramics fabricated from commercial TiB₂ powders. Hence, synthesizing TiB₂ from relatively inexpensive starting materials such as TiO₂, carbon, and B₄C emerges as a viable strategy to enhance the properties of B₄C ceramics.

On the fracture surfaces of the initial B₄C sintered sample (Fig. 7) and the sample containing 10 mol. % TiB₂ (Fig. 8, a), transgranular fracture of B₄C was

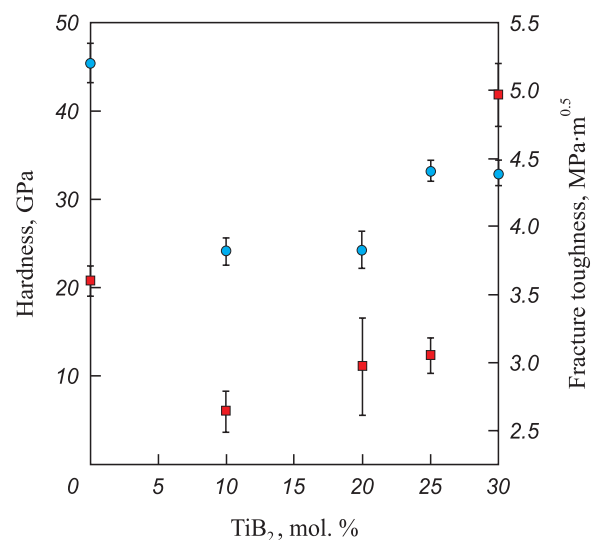


Fig. 6. Hardness (●) and fracture toughness (■) of composite ceramics as a function of amount of TiB₂ additive

Рис. 6. Твердость (●) и трещиностойкость (■) композиционной керамики в зависимости от количества добавки TiB₂

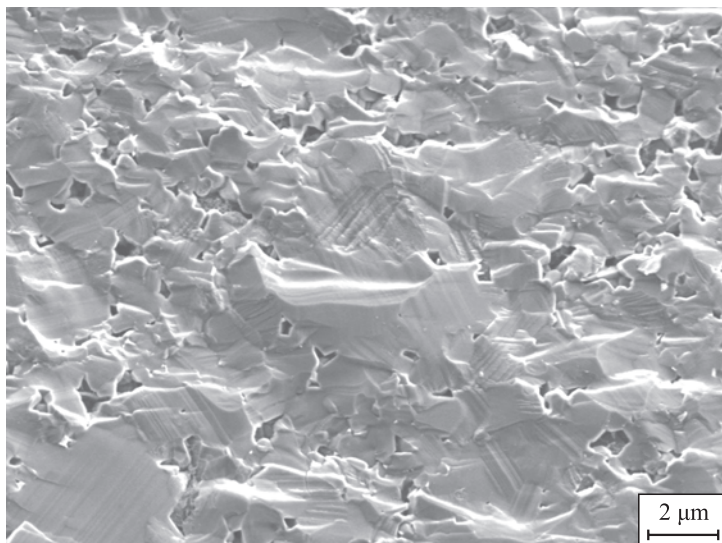


Fig. 7. Fracture surface of sintered B_4C without additives

Рис. 7. Поверхность разрушения спеченного B_4C без добавок

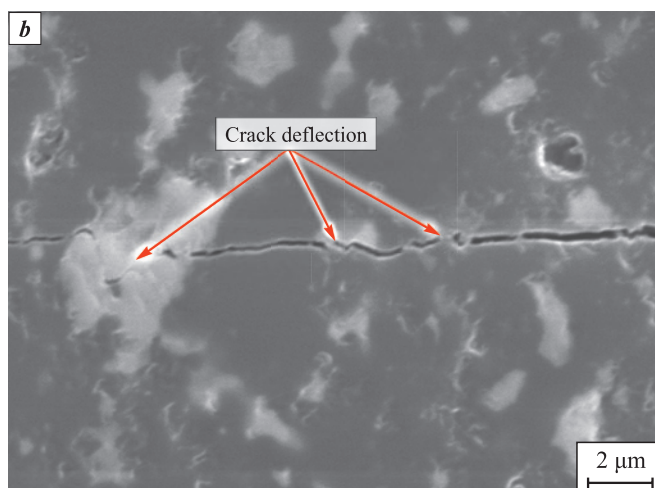
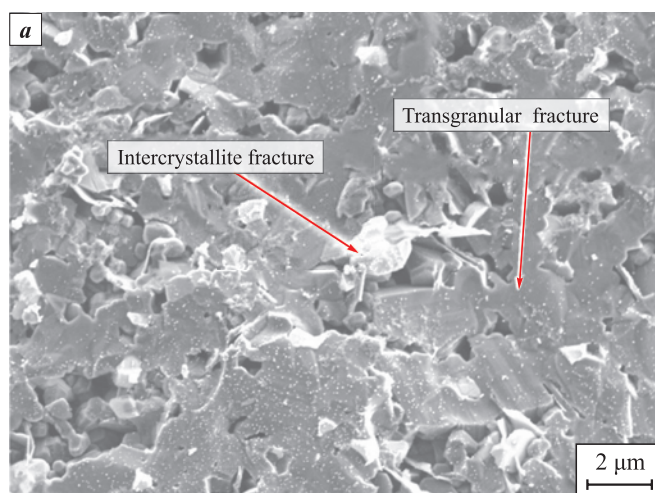


Fig. 8. Microstructure of ceramics with addition of 10 mol. % TiB_2
a – fracture surface, *b* – crack deflection on TiB_2 grains and agglomerates

Рис. 8. Микроструктура керамики с добавкой 10 мол. % TiB_2
a – поверхность разрушения, *b* – отклонение трещины на зернах и агломератах TiB_2

observed. This indicates a significantly strong cohesive strength among the intergranular bonds. According to ceramic materials fracture theory, the dominance of a transgranular fracture mechanism positively influences fracture toughness.

In certain TiB₂ grains, a variation in the fracture pattern within the intergranular regions is noted (Fig. 8, b). Similar observations were made in previous studies [15; 22], especially when a crack transitions from B₄C to TiB₂. Such variations could stem from alterations in the crack's path as it approaches grains possessing a fracture toughness superior to that of the B₄C matrix. This crack deflection process is likely to facilitate the dissipation of energy, thereby enhancing the mechanical properties of the composite ceramics [6]. In the examined material, such crack deflection was distinctly visible upon interaction with TiB₂ grains (refer to Fig. 8, b), accounting for the observed increase in fracture toughness in the composite with 30 mol. % TiB₂ in comparison to the additive-free B₄C.

Conclusions

The investigation has established clear trends in the alterations to the microstructure and properties of B₄C-based composite ceramics as a function of their composition.

1. X-ray phase analysis has verified that the sintered composite materials are composed of boron carbide and titanium diboride. The absence of TiO₂ reflections in the X-ray diffraction patterns substantiates the complete synthesis of TiB₂.

2. An increment in the TiB₂ content results in an enlarged average grain size of the diboride, with the formation of substantial clusters ranging between 100–320 μm. This phenomenon may contribute to increased anisotropy in the properties of the ceramics.

3. The prevalent fracture mechanism in B₄C is observed to be transgranular, while TiB₂ exhibits intergranular failure. This distinction underscores a modulation in the trajectory of cracks when encountering TiB₂ particles, where crack deviation is associated with the dissipation of energy, thereby enhancing the composite's fracture toughness.

4. The material incorporating 30 mol. % TiB₂ exhibits a synergy of high fracture toughness and hardness. This composition is distinguished by its elevated relative density, diminished open porosity, and a robust cohesive strength among grains.

References / Список литературы

1. Jianxin D. Erosion wear of boron carbide ceramic nozzles by abrasive air-jets. *Materials Science and Engineering A*.

2005;408(1-2):227–233.

<https://doi.org/10.1016/j.msea.2005.07.029>

2. Wang C., Lu Z., Zhang K. Microstructure, mechanical properties and sintering model of B₄C nozzle with microholes by powder injection molding. *Powder Technology*. 2012;228:334–338.

<https://doi.org/10.1016/j.powtec.2012.05.049>

3. Junlong S., Changxia L., Jin T., Baofu F. Erosion behavior of B₄C based ceramic nozzles by abrasive air-jet. *Ceramics International*. 2012;38(8):6599–6605.

<https://doi.org/10.1016/j.ceramint.2012.05.045>

4. Lee H., Speyer R. F. Hardness and Fracture Toughness of Pressureless-Sintered Boron Carbide (B₄C). *Journal of the American Ceramic Society*. 2002;85(5):1291–1293.

<https://doi.org/10.1111/j.1151-2916.2002.tb00260.x>

5. Yamada S., Hirao K., Yamauchi Y., Kanzaki S. High strength B₄C–TiB₂ composites fabricated by reaction hot-pressing. *Journal of the European Ceramic Society*. 2003;23(7):1123–1130.

[https://doi.org/10.1016/S0955-2219\(02\)00274-1](https://doi.org/10.1016/S0955-2219(02)00274-1)

6. Liu Y., Li Z., Peng Y., Huang Y., Huang Z., Zhan D. Effect of sintering temperature and TiB₂ content on the grain size of B₄C–TiB₂ composites. *Materials Today Communications*. 2020;23:100875.

<https://doi.org/10.1016/j.mtcomm.2019.100875>

7. Guo W., Wang A., He Q., Tian T., Liu C., Hu L., Shi Y., Liu L., Wang W., Fu Z. Microstructure and mechanical properties of B₄C–TiB₂ ceramic composites prepared via a two-step method. *Journal of the European Ceramic Society*. 2021;41(14):6952–6961.

<https://doi.org/10.1016/j.jeurceramsoc.2021.07.013>

8. Zhao S.M., Zhao L.R. Mechanical properties of hot-pressed B₄C–TiB₂ composites synthesized from B₄C–TiO₂ and B₄C–TiC. *Key Engineering Materials*. 2021;902:81–86.

<https://doi.org/10.4028/www.scientific.net/KEM.902.81>

9. Yuan Y., Ye T., Wu Y., Xu Y. Mechanical and ballistic properties of graphene platelets reinforced B₄C ceramics: Effect of TiB₂ addition. *Materials Science and Engineering: A*. 2021;817:141294.

<https://doi.org/10.1016/j.msea.2021.141294>

10. Ordan'yan S.S., Nesmelov D.D., Danilovich D.P., Udalov Yu.P. SiC–B₄C–Me^dB₂ systems and the prospects for creating composite ceramic materials based on them. *Powder Metallurgy and Functional Coatings*. 2016;(4):41–50. (In Russ.).

<https://doi.org/10.17073/1997-308X-2016-4-41-50>

Орданьян С.С., Несмелов Д.Д., Данилович Д.П., Удалов Ю.П. О строении систем SiC–B₄C–Me^dB₂ и перспективах создания композиционных керамических материалов на их основе. *Известия вузов. Порошковая металлургия и функциональные покрытия*. 2016;(4):41–50.

<https://doi.org/10.17073/1997-308X-2016-4-41-50>

11. Gunjishima I., Akashi T., Goto T. Characterization of directionally solidified B₄C–TiB₂ composites prepared by a floating zone method. *Materials Transactions*. 2002; 43(4):712–720. <https://doi.org/10.2320/matertrans.43.712>

12. Huang S.G., Vanmeensel K., Malek O.J.A., Van der Biest O., Vleugels J. Microstructure and mechanical properties of pulsed electric current sintered B₄C–TiB₂


- composites. *Materials Science and Engineering: A*. 2011;528(3): 1302–1309. <https://doi.org/10.1016/J.MSEA.2010.10.022>
13. Carter C.B., Norton M.G. Ceramic materials. New York: Springer, 2013. 766 p.
 14. Skorokhod V.V., Krstic V.D. Processing, microstructure, and mechanical properties of B_4C-TiB_2 particulate sintered composites. II. Fracture and mechanical properties. *Powder Metallurgy and Metal Ceramics*. 2000;39(9):504–513. <https://doi.org/10.1023/A:1011378825628>
 15. Dai J., Pineda E.J., Bednarczyk B.A., Singh J., Yamamoto N. Macro-scale testing and micromechanics modeling of fracture behaviors for boron carbide composites with hierarchical microstructures. In: *AIAA Scitech 2021 Forum* (11–15 and 19–21 January 2021). USA, American Institute of Aeronautics and Astronautics, 2021. P. 14. <https://doi.org/10.2514/6.2021-0405>
 16. Skorokhod V., Krstic V.D. High strength-high toughness B_4C-TiB_2 composites. *Journal of Materials Science Letters*. 2000;19(3):237–239. <https://doi.org/10.1023/A:1006766910536>
 17. Ivanov Y.F., Khasanov O.L., Polisadova V.V., Petyukovich M.S., Milovanova T.V., Teresov A.D., Bikbaeva Z.G., Kalashnikov M.P., Bratukhina A.S. The analysis of the mechanisms for plasticization of boron carbide ceramics irradiated by an intense electron beam. *Key Engineering Materials*. 2016;685:700–704. <https://doi.org/10.4028/www.scientific.net/KEM.685.700>
 18. Yue X.Y., Zhao S.M., Yu L., Ru H.Q. Microstructures and mechanical properties of B_4C-TiB_2 composite prepared by hot pressure sintering. *Key Engineering Materials*. 2010;34:50–53. <https://doi.org/10.4028/www.scientific.net/KEM.434-435.50>
 19. Yue X.Y., Zhao S.M., Lü P., Chang Q., Ru H.Q. Synthesis and properties of hot pressed B_4C-TiB_2 ceramic composite. *Materials Science and Engineering: A*. 2010;527(27-28):7215–7219. <https://doi.org/10.1016/J.MSEA.2010.07.101>
 20. Liu A.D., Qiao Y.J., Liu Y.Y. Pressureless sintering and properties of boron carbide-titanium diboride composites by *in situ* reaction. *Key Engineering Materials*. 2012;525:321–324. <https://doi.org/10.4028/www.scientific.net/KEM.525-526.321>
 21. Li A., Zhen Y., Yin Q., Ma L., Yin Y. Microstructure and properties of $(SiC, TiB_2)/B_4C$ composites by reaction hot pressing. *Ceramics International*. 2006;32(8):849–856. <https://doi.org/10.1016/j.ceramint.2005.05.022>
 22. Skorokhod V.V., Krstic V.D. Processing, microstructure, and mechanical properties of B_4C-TiB_2 particulate sintered composites. Part I. Pressureless sintering and microstructure evolution. *Powder Metallurgy and Metal Ceramics*. 2000;39(7):414–423. <https://doi.org/10.1023/A:1026625909365>
 23. Wang Y., Peng H., Ye F., Zhou Y. Effect of TiB_2 content on microstructure and mechanical properties of in-situ fabricated TiB_2/B_4C composites. *Transactions of Nonferrous Metals Society of China*. 2011;21:369–373. [https://doi.org/10.1016/S1003-6326\(11\)61608-7](https://doi.org/10.1016/S1003-6326(11)61608-7)
 24. Gudyma T.S., Krutskii Y.L., Maksimovskii E.A., Ukhina A.V., Aparnev A.I., Smirnov A.I., Uvarov N.F. Synthesis of B_4C/ZrB_2 composite powders via boron carbide reduction for ceramic fabrication. *Inorganic Materials*. 2022;58(9):912–921. <https://doi.org/10.1134/S0020168522090059>
 25. Krutskii Y.L., Bannov A. G., Sokolov V.V., Dyukova K.D., Shinkarev V.V., Ukhina A.V., Maksimovskii E.A., Pichugin A.Yu., Solov'ev E.A., Krutskaya T.M., Kuvshinov G.G. Synthesis of highly dispersed boron carbide from nanofibrous carbon. *Nanotechnologies in Russia*. 2013;8(3): 191–198. <https://doi.org/10.1134/S1995078013020109>
 Крутский Ю.Л., Баннов А.Г., Соколов В.В., Дюкова К.Д., Шинкарев В.В., Ухина А.В., Максимовский Е.А., Пичугин А.Ю., Соловьев Е.А., Крутская Т.М., Кувшинов Г.Г. Синтез высокодисперсного карбида бора из нановолокнистого углерода. *Российские нанотехнологии*. 2013;8(3-4):43–48
 26. Kurmashov P.B., Maksimenko V.V., Bannov A.G., Kuvshinov G.G. Horizontal vibrofluidized bed pilot reactor for nanofibrous carbon synthesis process. *Khimicheskaya tehnologiya*. 2013;14(10):635–640. (In Russ.).
 Курмашов П.Б., Максименко В.В., Баннов А.Г., Кувшинов Г.Г. Горизонтальный пилотный реактор с виброожиженным слоем для процесса синтеза нановолокнистого углерода. *Химическая технология*. 2013;14(10):635–640.
 27. Krutskii Y.L., Krutskaya T.M., Gudyma T.S., Gerasimov K.B., Khabirov R.R., Mass A.V. Carbothermal and boron carbide reduction of oxides of some transition metals. In: *Proceedings of VII International Russian–Kazakhstan Conference «Chemical Technologies of Functional Materials»* (Novosibirsk, Russia, 28–30 April 2021). MATEC Web of Conferences, 2021. P. 01040. <https://doi.org/10.1051/mateconf/202134001040>
 28. Angers R., Beauvy M. Hot-pressing of boron carbide. *Ceramics International*. 1984;10(2):49–55. [https://doi.org/10.1016/0272-8842\(84\)90025-7](https://doi.org/10.1016/0272-8842(84)90025-7)
 29. Hwang C., DiPietro S., Xie K.Y., Yang Q., Celik A.M., Khan A.U., Domnich V., Walck S., Hemker K.J., Haber R.A. Small amount TiB_2 addition into B_4C through sputter deposition and hot pressing. *Journal of the American Ceramic Society*. 2019;102(8):4421–4426. <https://doi.org/10.1111/jace.16457>
 30. He P., Dong S., Kan Y., Zhang X., Ding Y. Microstructure and mechanical properties of B_4C-TiB_2 composites prepared by reaction hot pressing using Ti_3SiC_2 as additive. *Ceramics International*. 2016;42(1A):650–656. <https://doi.org/10.1016/j.ceramint.2015.08.160>
 31. Thevenot F. Boron carbide – A comprehensive review. *Journal of the European Ceramic Society*. 1990;6(4): 205–225. [https://doi.org/10.1016/0955-2219\(90\)90048-K](https://doi.org/10.1016/0955-2219(90)90048-K)
 32. Tee K.L., Lu L., Lai M.O. In situ processing of $Al-TiB_2$ composite by the stir-casting technique. *Journal of Materials Processing Technology*. 1999;89-90:513–519. [https://doi.org/10.1016/S0924-0136\(99\)00038-2](https://doi.org/10.1016/S0924-0136(99)00038-2)
 33. Yi H., Ma N., Zhang Y., Li X., Wang H. Effective elastic moduli of $Al-Si$ composites reinforced in situ with TiB_2 particles. *Scripta Materialia*. 2006;54(6):1093–1097. <https://doi.org/10.1016/j.scriptamat.2005.11.070>
 34. Khasanov A.O. Development of compositions and technology of spark-plasma sintering of ceramic materials, composites based on micro- and nanopowders B_4C : Diss. Cand Sci. (Eng.). Tomsk: TPU, 2015. (In Russ.).

- Хасанов А.О. Разработка составов и технологии спарк-плазменного спекания керамических материалов, композитов на основе микро- и нанопорошков B₄C: Дис. ... канд. техн. наук. Томск: ТПУ, 2015.
35. Niihara K., Morena R., Hasselman D.P.H. Evaluation of K_{Ic} of brittle solids by the indentation method with low crack-to-indent ratios. *Journal of Materials Science Letters*. 1982;1(1):13–16.
<https://doi.org/10.1007/BF00724706>
36. Khasanov O.L., Struts V.K., Sokolov V.M., Polisadova V.V., Dvilis E.S., Bikbaeva Z.G. Methods for measuring microhardness and crack resistance of nanostructured ceramics. Tomsk: Publishing House of Tomsk Polytechnic University, 2011. 101 p. (In Russ.).
 Хасанов О.Л., Струц В.К., Соколов В.М., Полисадова В.В., Двилис Э.С., Бикбаева З.Г. Методы измерения микротвердости и трещиностойкости наноструктурных керамик. Томск: Изд-во Томского политехнического университета, 2011. 101 с.
37. Chen D., Zhang K., Zeng J., Guo H., Li B. High-strength TiB₂–B₄C composite ceramics sintered by spark plasma sintering. *International Journal of Applied Ceramic Technology*. 2022;19(4):1949–1955.
<https://doi.org/10.1111/ijac.14051>
38. Liu Z., Deng X., Li J., Sun Y., Ran S. Effects of B₄C particle size on the microstructures and mechanical properties of hot-pressed B₄C–TiB₂ composites. *Ceramics International*. 2018;44(17):21415–21420.
<https://doi.org/10.1016/j.ceramint.2018.08.200>
39. Yaşar Z. A., Celik A.M., Haber R.A. Improving fracture toughness of B₄C–SiC composites by TiB₂ addition. *International Journal of Refractory Metals and Hard Materials*. 2022;108:105930.
<https://doi.org/10.1016/j.ijrmhm.2022.105930>

Information about the Authors

Сведения об авторах

Roman R. Khabirov – Postgraduate Student at the Department “Materials Science in Mechanical Engineering”, Novosibirsk State Technical University (NSTU)

 ORCID: 0000-0003-4720-2876


 E-mail: xabirov.2016@stud.nstu.ru

Nina Yu. Cherkasova – Cand. Sci. (Eng.), Junior Researcher of the Research Laboratory of Physical and Chemical Technologies and Functional Materials, NSTU

 ORCID: 0000-0002-5603-7852


 E-mail: cherkasova.2013@corp.nstu.ru

Tatiana S. Gudyma – Junior Researcher of the Laboratory of Chemical Technology of Functional Materials, NSTU

 ORCID: 0000-0002-4724-3371

 E-mail: gudymatan@mail.ru

Yurii L. Krutskii – Dr. Sci. (Eng.), Associate Professor at the Department of Chemistry and Chemical Technology, NSTU

 ORCID: 0000-0003-2524-4143


 E-mail: krutskij@corp.nstu.ru

Anna V. Mass – Postgraduate Student at the Department “Materials Science in Mechanical Engineering”, NSTU

 ORCID: 0000-0003-2053-7422


 E-mail: a.mass@corp.nstu.ru

Tatiana S. Ogneva – Cand. Sci. (Eng.), Senior Researcher of the Research Laboratory of Physical and Chemical Technologies and Functional Materials, NSTU

 ORCID: 0000-0002-0081-283X


 E-mail: ogneva@corp.nstu.ru

Ruslan I. Kuzmin – Cand. Sci. (Eng.), Junior Researcher at the Center for Technological Excellence, NSTU

 ORCID: 0000-0001-7712-4296

 E-mail: kuzmin.2010@corp.nstu.ru

Alexander G. Anisimov – Cand. Sci. (Phys.-Math.), Senior Researcher of the Laboratory “Synthesis of Composite Materials”, Lavrentyev Institute of Hydrodynamics of the Siberian Branch of the Russian Academy of Sciences

 ORCID: 0000-0002-0244-2246


 E-mail: anis@hydro.nsc.ru

Роман Рафаэлович Хабиров – аспирант кафедры материаловедения в машиностроении, Новосибирский государственный технический университет (НГТУ)

 ORCID: 0000-0003-4720-2876

 E-mail: xabirov.2016@stud.nstu.ru

Нина Юрьевна Черкасова – к.т.н., мл. науч. сотрудник научно-исследовательской лаборатории физико-химических технологий и функциональных материалов, НГТУ

 ORCID: 0000-0002-5603-7852

 E-mail: cherkasova.2013@corp.nstu.ru

Татьяна Сергеевна Гудыма – мл. науч. сотрудник лаборатории химической технологии функциональных материалов, НГТУ

 ORCID: 0000-0002-4724-3371

 E-mail: gudymatan@mail.ru

Юрий Леонидович Крутский – д.т.н., доцент кафедры химии и химической технологии, НГТУ

 ORCID: 0000-0003-2524-4143


 E-mail: krutskij@corp.nstu.ru

Анна Владимировна Масс – аспирант кафедры материаловедения в машиностроении, НГТУ

 ORCID: 0000-0003-2053-7422


 E-mail: a.mass@corp.nstu.ru

Татьяна Сергеевна Огнева – к.т.н., ст. науч. сотрудник научно-исследовательской лаборатории физико-химических технологий и функциональных материалов, НГТУ

 ORCID: 0000-0002-0081-283X


 E-mail: ogneva@corp.nstu.ru

Руслан Изатович Кузьмин – к.т.н., мл. науч. сотрудник Центра технологического превосходства, НГТУ

 ORCID: 0000-0001-7712-4296

 E-mail: kuzmin.2010@corp.nstu.ru

Александр Георгиевич Анисимов – к.ф.-м.н., ст. науч. сотрудник лаборатории синтеза композиционных материалов, Институт гидродинамики им. М.А. Лаврентьева СО РАН

 ORCID: 0000-0002-0244-2246

 E-mail: anis@hydro.nsc.ru

Contribution of the Authors**Вклад авторов**

R. R. Khabirov – formulated the main concept, defined the goal and objectives of the work, conducted experiments, processed and analyzed the study results, and wrote the manuscript

N. Yu. Cherkasova – formulated the main concept, defined the goal and objectives of the work, conducted structural studies, and wrote the manuscript.

T. S. Gudyma – formulated the main concept, defined the goal and objectives of the work, synthesized powder mixtures, and wrote the manuscript.

Yu. L. Krutskii – provided scientific management and conducted experiments.

A. V. Mass – conducted structural studies and participated in the discussion of the results.

T. S. Ogneva – carried out X-ray phase analysis and participated in the discussion of the results.

R. I. Kuzmin – conducted experiments and participated in the discussion of the results.

A. G. Anisimov – conducted experiments and participated in the discussion of the results.

Р. Р. Хабиров – формирование основной концепции, постановка цели и задач работы, проведение экспериментов, обработка и анализ результатов исследования, составление текста статьи.

Н. Ю. Черкасова – формирование основной концепции, постановка цели и задач работы, проведение структурных исследований, написание текста статьи.

Т. С. Гудыма – формирование основной концепции, постановка цели и задач работы, синтез порошковых смесей, написание текста статьи.

Ю. Л. Крутский – научное руководство, проведение экспериментов.

А. В. Масс – проведение структурных исследований, участие в обсуждении результатов.

Т. С. Огнева – проведение рентгенофазового анализа, участие в обсуждении результатов.

Р. И. Кузьмин – проведение экспериментов, участие в обсуждении результатов.

А. Г. Анисимов – проведение экспериментов, участие в обсуждении результатов.

Received 08.12.2022
Revised 19.07.2023
Accepted 22.07.2023

Статья поступила 08.12.2022 г.
Доработана 19.07.2023 г.
Принята к публикации 22.07.2023 г.